Design and Implementation of a 250W, Low Speed Switched Reluctance Hub Motor

[1]V.Chandrasekar, [2]S.Prabhu, [3]R.Arumugam,
[1,]Asst. Professor, Arunai Engineering College, Tiruvannamalai, India,
[3]Former Professor, Anna University, SSN Engineering College, Chennai, India
Vcsekar75@yahoo.co.in

Abstract— **This paper aims at design, analytical verification, fabrication and implementation of a 250 W, 200 rpm, 48 V, 8/6 pole, SR Hub motor. Step by step procedure for SR hub motor is presented. The procedure is evolved from the basic background in electromagnetics. Subsequently Finite Element software is used to analyse the machine parameters. With design parameters, aligned inductance, and unaligned inductances are calculated, measured and compared with FEA results. The machine is fabricated and the commutation schemes for SR Hub motor are presented. This scheme permits a simple logic control and with position feedback from a new low-resolution position sensors.**

***Keywords*— Design of Switched Reluctance Hub motor, Finite Element Analysis, Commutation of SR Hub Motor.**

1. INTRODUCTION

In today's world various factors such as, rising fossil fuel cost, slow regeneration of renewable energy sources and several environmental concerns have stimulated the trend of electrical vehicle. Unlike conventional drive system, torque as well as the power and speed can be directly supplied to the tyre using a Hub motor. This arrangement eliminates the gear and need for mechanical differentials.

In present electric vehicle direct drive system, the brushless dc (BLDC) motor is the hub motor of choice. However, the higher cost of rare-earth permanent magnets and the complexity of its controller are some of its disadvantages. [4] Outer-rotor type multi polar switched reluctance motor is simple in construction and robust. The recent advances in power electronics technology have made switched reluctance Hub motor suited for many of the emerging applications for electric drive system. Since the torque is proportional to the square of the current, this machine resembles a dc series motor; hence it has a good starting torque. The machine is suitable for four quadrant operation with a converter. [5]

The procedure of design of switched reluctance machine starts with selection of a frame size and progresses to the selection various dimensions in a methodical manner. [6] A step by step procedure has been developed for the design of SR motor and output equation is developed in a manner similar to that used for conventional rotating machines, [2]. With the selection of dimensions, a procedure to calculate the inductance in the aligned and unaligned position is outlined [6], [10]. Design and analysis of SR motor in electric vehicle has been done in [4], [7] – [9], [11] – [16]. Design procedure for SR hub motor with Nr=Ns+2 is given in [4], [9]. But, design procedure for a SR hub motor with $N_r=N_s-2$ is dealt in this paper.

This paper shows the design procedure for the switched reluctance hub motor initializing by choosing bore diameter and stack length. After selecting all required dimensions, the procedure to calculate aligned and unaligned inductance is done. This paper shows the designer to use the concept of electromagnetic, to design a SR hub motor with $N_r=N_s-2$.

Paper is organised on the following lines: Section 2 contains design procedure for SR Hub Motor. Verification of the design, based on Finite Element Analysis is discussed in section 3. Commutation sequences and current waveforms are discussed in section 4. Section 5 contains the conclusion.

2. DESIGN PROCEDURE

Design methodology of an In-hub mini-SR motor for the spindle motor in 3.5" hard disc drive is presented in [4]. Torque is calculated using a hybrid method, combining the solutions of FEM analysis with the time-stepping integration of the output equation. It was an 8 stator poles and 10 rotor poles machine. The absolute torque zone is 18^0, Time period during one working stroke is 15 ms.

There is always choice of having either $N_r=N_s-2$, as in the 8/6; or $N_r=N_s+2$, as in the 8/10. The disadvantage of the larger N_r is lower inductance ratio which may increase the controller volt-amperes and decrease the specific output. The 8/10 pole structure motor has 40 strokes/rev and inductance ratio is inevitably lower than in the 8/6: the poles are narrower, while the clearance between pole corners in the unaligned position is smaller, increasing the unaligned inductance. [3] Table 1 shows the comparison of parameters between 8/10 and 8/6 pole combinations. The procedure outlined here has been derived in detail in [6] for conventional SR motor. Additionally, there is an attempt to derive equations, to bring the windings to inner part of the machine.

The design of switched Reluctance Hub motor needs to comply with diameter restrictions due to housing the motor in wheel rim so that it can achieve the compactness. Hence the peripheral length of the machine is restricted to 700 mm. This paper attempts to modify the design procedure described in [6]. The design of switched Reluctance Hub motor needs to comply with diameter restrictions due to housing the motor in wheel rim so that it can achieve the compactness. Hence the peripheral length of the machine is restricted to 700 mm. This paper attempts to modify the design procedure described in [6]. The design modification has been done according to the requirements of the manufactures which will help manufacture of SR hub motor with not enough knowledge in design of SR hub motor to build and to test the prototype model.

Table 1 Comparison between 8/10 and 8/6 Pole structure

Parameter	8/10	8/6
Stroke angle	9^0	15^0
Absolute torque zone	18^0	30^0
Time for one working stroke	15 ms	25 ms
Frequency of excitation of one phase	33.33 Hz	20 Hz
Profile of torque	Not flat top	Flat top

2.1 Machine Specifications

Output power = 250W
Rated speed = 200 rpm
Peake value of current = 7.5A
Supply voltage = 48V
Torque required is given by

$$T_{req} = \frac{P_{kw}}{\frac{2\pi N}{60}} \quad \text{Nm} \qquad (1)$$

Where P_{kw} is power output in Watts
N is speed in rpm

***2.2* Selection of Pole arcs**

Initially, stator pole angle must be lesser than the rotor pole angle for better torque production.

$$\beta_s < \beta_r \qquad (2)$$

Then, Stroke angle is the angle through which the rotor moves for excitation of single phase excitation with supply current.

$$\text{Stroke angle, } \varepsilon = \frac{4\pi}{N_s N_r} = 15^0 \qquad (3)$$

Finally,

$$\beta_s < \frac{2 * \pi}{N_r} - \beta_r \qquad (4)$$

$$\beta_s + \beta_r \le 60^0 \qquad (5)$$

2.3 Preliminary Design Process

The bore diameter and stack length can be initially chosen. With the selection of Do, L, D, β_s and β_r the design process is continued. The shaft diameter D_{sh} can also be selected from the IEC regulations. Diagrammatic representation of proposed analytical model of SR Hub Motor is shown in Fig.1.

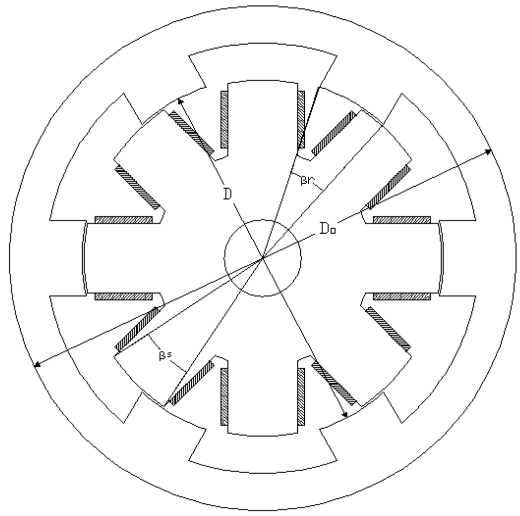

Fig1: SR hub motor

Stack Length of the machine D = 75 mm (6)

It is chosen that stator pole angle; $\beta_r = 24^o$ and rotor pole angle; $\beta s = 22^o$.Frame size of the machine; D = 165 mm, D_0=233mm.It is assumed that the stator pole flux density is equal to that of maximum flux density.

$$B_s = B_{max} = 1.1215T. \qquad (7)$$

The stator pole area can be written as just by eliminating the leakage and stack factor,

$$A_s = (\frac{D}{2} - g) L \beta_s \qquad (8)$$

Flux in the stator pole can be written as

$$\phi = B_S * A_S = 0.00222 \text{ Wb} \qquad (9)$$

Flux in the yoke can be written as,

$$\Phi_y = \frac{\Phi}{2} = 0.000111\text{Wb} \qquad (10)$$

Rotor Pole Area is given by;

$$A_r = (\frac{D}{2}) L \beta_r \qquad (11)$$

Here the area of the yoke is equal to the area of the rotor is given by;

$$A_y = Ar = C*L \qquad (12)$$

The rotor back iron thickness is given by

$$C = \frac{A_y}{L} \qquad (13)$$

The yoke flux density is given by;

$$B_y = \frac{\phi_y}{A_y} \quad (14)$$

Area of stator core,

A_{sc}=As/1.6= 0.00130m^2 (15)

Stator pole height,

$$h_s = \frac{D}{2} - g - \frac{D_{sh}}{2} - \frac{A_{sc}}{L} \quad (16)$$

Here,

$A_r B_r = A_S B_S$ (17)

The flux density in the rotor pole is given by;

$$B_r = \frac{B_s A_s}{A_r} \quad (18)$$

Taking , D_{sh} = 80 mm. The stator pole height is given as;

$$h_s = \frac{D_o}{2} - C - \frac{D}{2} \quad (19)$$

Neglecting leakage and fringing, Air gap area

$$A_g = \left[\frac{D}{2} - \frac{g}{2}\right]\left[\frac{\beta_r + \beta_s}{2}\right] * \frac{\pi}{180} * 75 * 10^{-6} m^2 \quad (20)$$

The flux density in the air gap is given by;

$$B_g = \frac{A_s B_s}{A_g} = 1.0908T \quad (21)$$

The magnetic flux density in the air gap is given by;

$$H_g = \frac{B_g}{4\pi * 10^{-7}} \quad (22)$$

The flux density in the stator core is given by;

$$B_{sc} = \frac{\phi_{sc}}{A_{sc}} \quad (23)$$

Area of the stator core is given by;

$$A_{sc} = \frac{A_r}{1.6} \quad (24)$$

The length of the flux path in rotor,

$$l_r = h_r + \frac{c}{2} \quad (25)$$

The length of the flux path in stator,

$$ls = \frac{D}{4} - \frac{g}{2} + \frac{h_s}{2} + \frac{D_{sh}}{4} \quad (26)$$

The length of the flux path in stator core,

$$l_{sc} = \pi * \left[\frac{D}{4} - \frac{g}{2} - \frac{h_s}{2} + \frac{D_{sh}}{4}\right] \quad (27)$$

The length of the flux path in yoke;

$$l_y = \pi * \left[\frac{D_o}{2} - \frac{C}{2}\right] \quad (28)$$

The mmf drop equation obtained is,

$$S = T_{ph} i_p = 2*(H_s l_s + H_g l_g + H_r l_r) + \frac{H_{sc} l_{sc}}{2} + \frac{H_y l_y}{2} \quad (29)$$

2.3 Winding Design

Number of turns per phase is given by;

$$T_{ph} = \frac{S}{i_p} \quad (30)$$

Stator pole pitch is given by;

$$\lambda_s = \frac{(\frac{D}{2} - G - h_s)2\pi}{Ns} \quad (31)$$

Let wedge thickness = 4mm.then Stator pole arc length is given by;

$$t_s = \left(\frac{D}{2} - g\right)\beta_s \quad (32)$$

Let the minimum area of the conductor when ;j=7A/mm^2 is,

$$a_c = \frac{i}{j\sqrt{q}} \quad (33)$$

Diameter of coil is given by;

$$d_c = \sqrt{\frac{4a_c}{\pi}} \quad (34)$$

Nearby standard size conductor is SWG 20, with d_c = 0.914 mm. Maximum height of the winding; h_w = 4mm.number of horizontal layers is given by;

$$N_{tlayer} = \frac{h_w f_f}{d_w} \quad (35)$$

Number of vertical layer is given by;

$$N_{layer} = \frac{T_{ph}}{2 * N_{tlayer}} \quad (36)$$

Width of the winding is given by;

$$W_t = \frac{d_w N_{layer}}{f_f} \quad (37)$$

Space between two stator pole tips at the base of the windings

$$Z = \lambda_s - t_s \quad (38)$$

Clearance between the windings at the bore

$$cl = Z - 2*W_t \tag{39}$$

2.5 Calculation of inductances

The aligned inductances is,

$$L_a = \frac{T_{ph} * \phi}{i_p} \tag{40}$$

Minimum inductance is calculated by plotting the equiflux tubes for the machine in the unaligned rotor position and calculate the lengths of the equiflux lines in vacuum and then account for the paths in the iron portions[5], [6]. The total unaligned inductance Lu is,

$$L_u = L_{u1} + 2(L_{u2} + L_{u3} + L_{u4} + L_{u5} + L_{u6} + L_{u7}) + 4(L_{u8} + L_{u9} + L_{u10}) \tag{41}$$

2.6 Calculation of average torque

The average torque developed by the machine is

i. After equating the S_{act} with S_{cal}, Bs1, and Bs2….Bsn can be obtained.
ii. From Bs1, Bs2….Bsn, the flux φ1, φ2…. Φn are found.
iii. Further the flux linkages λ1, λ2… λn, are obtained. The λ_a can then be plotted against various currents shown in Fig.2.
iv. The Unaligned inductance does not change with varying currents and so the unaligned flux linkages can be obtained at various currents above as $\lambda_{u1} = L_u * i_1$ and so on till the rated current and is plotted in Fig.2.

Net work done W from the Fig.4. is calculated as shown below.

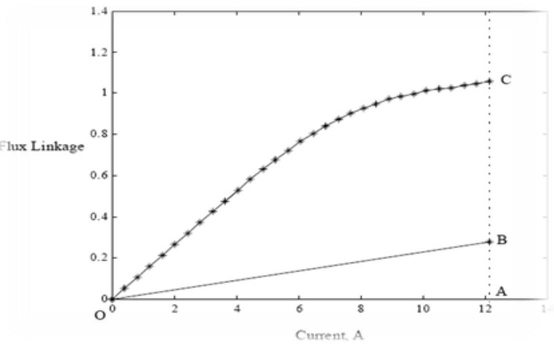

Fig:2 λ-i curve

$$W_{aligned} = \partial i(\lambda_1 + \lambda_2 + ... + \lambda_{n-1}) + \frac{\lambda_n \partial i}{2} \tag{42}$$

$$W_{aligned} = 0.5*(i_p{}^2 * L_u) \tag{43}$$

$$W = W_{align} - W_{unalign} = \text{Area OBCO} \tag{44}$$

$$Tav = \frac{WN_s Nr}{4\pi} \tag{45}$$

Where W = total work done

If the average torque calculated above is less than the required torque then some machine parameters have to be redesigned. The current can also be increased provided the designer is satisfied that the machine does not go into the saturation. This iteration is done till the designer is satisfied with the average developed torque value.

3. Design verification by finite element analysis

Finite Element Analysis (FEA) is used to calculate the torque produced at various currents and rotor positions as well as to calculate the phase inductances. The assumptions made in [6] to calculate various parameters for design verification by finite element method are followed in this paper also.

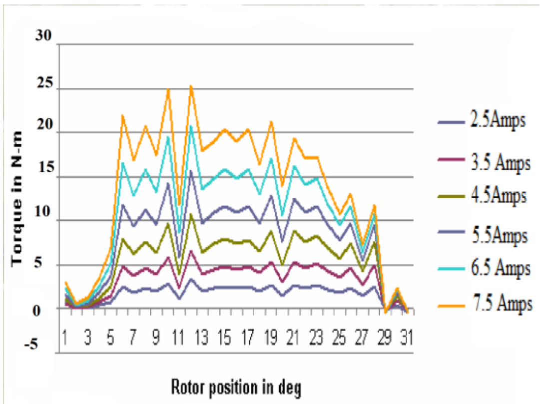

Fig3: Torque Vs Rotor position for various currents

Fig.3 shows the positive torque profile of 'A' phase, for various stator phase windings. Torque is almost flat from 6^0 of rotor position to 24^0 of rotor position. Fig 4 shows torque vs rotor position for all four phases. It is found that the positive and negative envelopes of the torque are ripple free. Fig. 5 shows that the rotor reaches one revolution in 300 ms. Fig 6 and Fig. 7 shows the flux tubes of the machine during aligned and the unaligned positions.

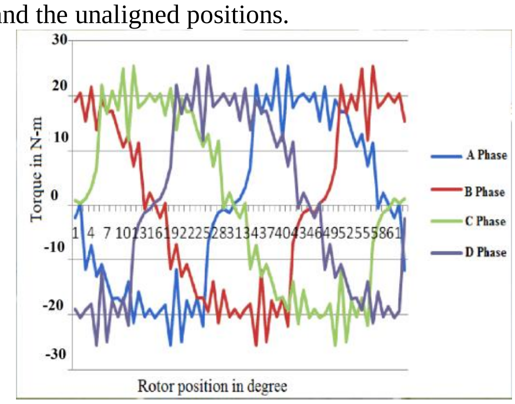

Fig4: Torque Vs Rotor position for all phases

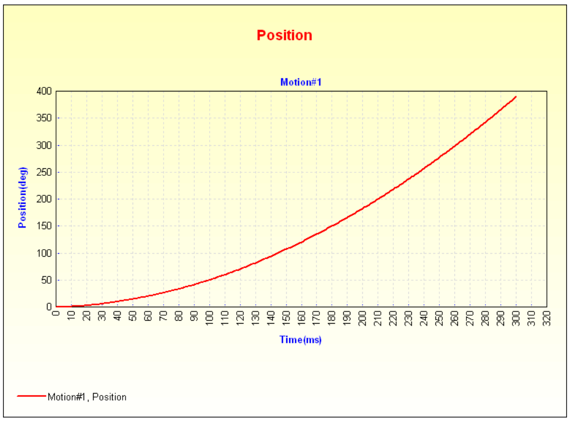

Fig 5: Rotor position Vs Time plot

Equiflux lines of an 8/6 SRM hub in the aligned position and unaligned position [4] shown in Fig.5.and Fig.6 respectively

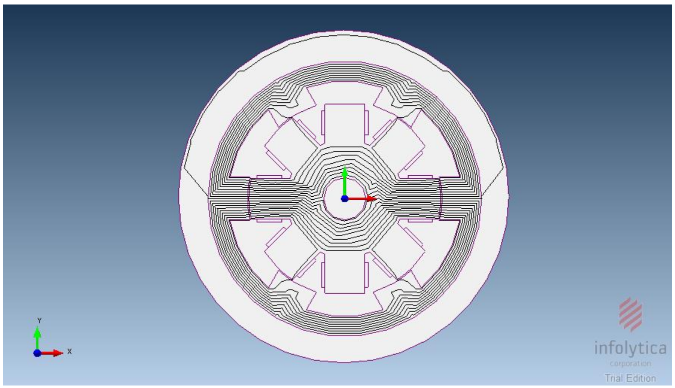

Fig 6: Flux path in alligned position

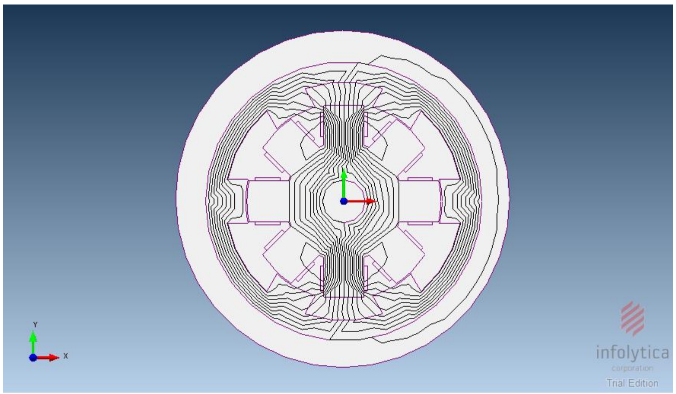

Fig 7: Flux path in Un-aligned position

4. Commutation in SR Hub Motor

Complex schemes use either position feedback from high-resolution position sensors or extensive circuitry for controlling the commutation parameters on a SR motor have been used. [3], [17] A scheme has been explained in [3], for generation of shaft position signals. This method cannot be used in SR hub motor, because, the shaft, which is connected to the centre of the hub motor, will not rotate. A new scheme with a sticker, stuck on the frame of SR hub motor can be used to sense the position of rotor. Fig ------- shows the sensor and commutation wave forms and some of the firing angle combinations. The prototype model has been developed for the designed dimensions.

4.1 Asymmetric Power Converter

Fig. 9 shows the block diagram of the controller used for SR hub motor. Various types of power converters are dealt in [5]. Asymmetric power converter, shown in fig. 10 is implemented for the control of SR hub motor. A phase winding is excited if PWM signal and the commutation signal are given to the upper and the lower switches of the converter respectively. The lower devices T2, T4, T6, and T8 are controlled from signals obtained by chopping frequency signal.

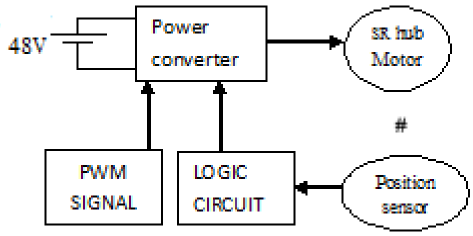

Fig. 9 Block diagram of Controller

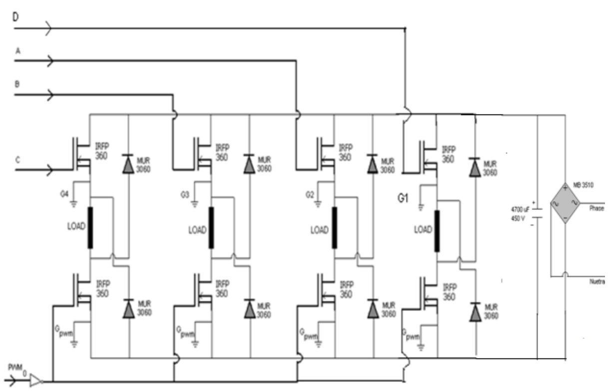

Fig10: Power Controller

4.2 Commutation Control

While the motor is set in rotation, the output signals of the four reflective sensors P, Q, R, S acts as the basic information of the rotor position, which has the phase difference of 15^0. Reflective sensors, mounted on the motor frame and a black and white coloured paper stuck on the rotor frame were used here. Four phase motors can be operated with two or four sensors. But four quadrant operation is possible only with four sensors. Number of steps per electrical rotation is n.

$$n = N_r q = 24 \qquad (46)$$

$$\theta_{step} = \frac{2\pi}{qN_r} = 15^0 \quad (47)$$

$$\theta_{res} = \frac{\pi}{SN_r} = 7.5^0 \quad (48)$$

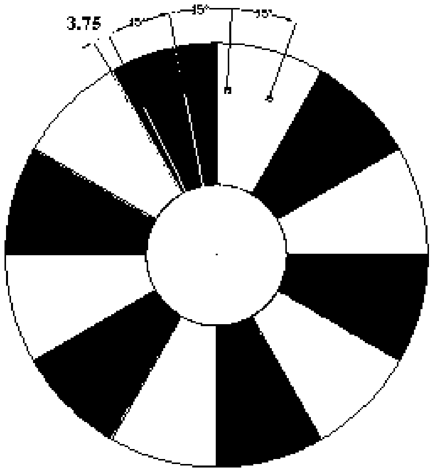

Fig. 11 Black and White coloured paper used as position sensor

Forward and reverse operations require precise adjustment of the conduction angles in reference to the rotor position. This is accomplished by placing position sensor at a specified angular distance $\theta_{P-shift}$ from the rotor position frame.

$$\theta_{P-shift} = \frac{\theta_{res}}{2} = 3.75^0$$

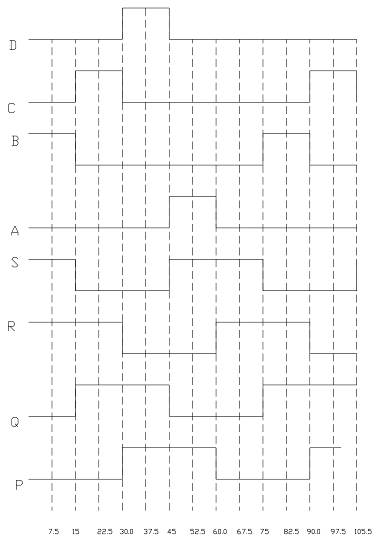

Fig 12 Commutation schemes

A shaft position sensor provides commutation signalsA, B, C, D as shown in fig. 11. Combinational logic derives the phase firing signals from the sensor signals. The motor current is controlled by chopping the upper transistors in fig 10. Position sensor signals and commutation signals are given in Fig. 12. Only the commutation signals are applied to the upper transistors. Fig13 shows different phase current wave forms.

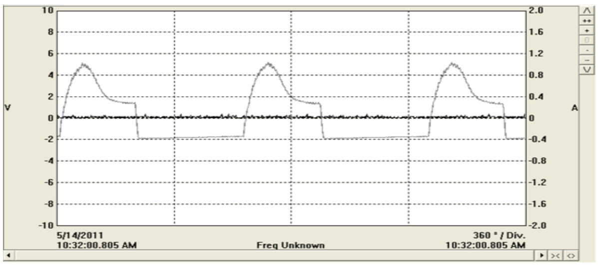

Fig13 (a): phase A current

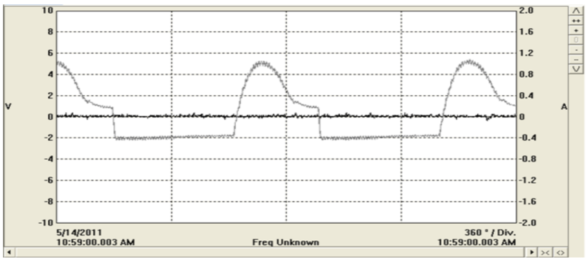

Fig13 (b): Phase B current

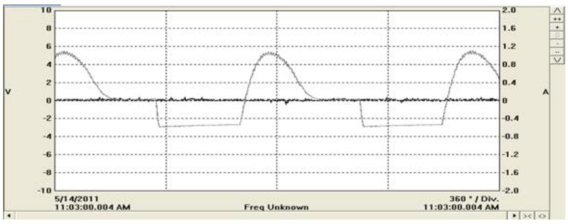

Fig13(c): Phase C current

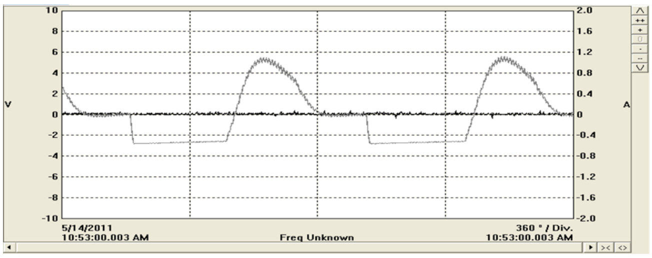

Fig13 (d): Phase D current

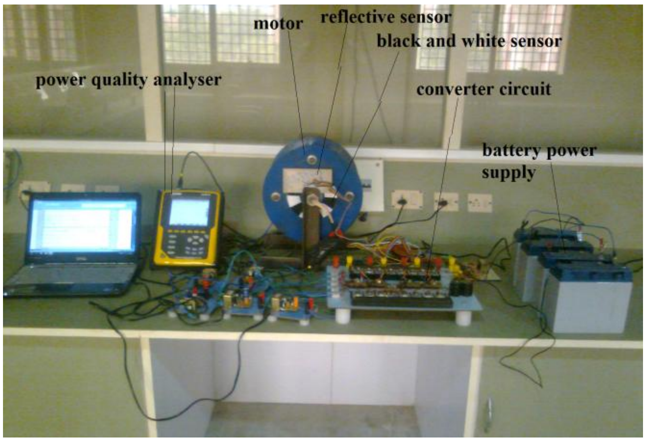

Fig14: Switched Reluctance Hub Motor with Position sensor

Table2: Rotor Position and Gating Signals

Rotor Position	Sensor O/P				Gating Signals			
	P	Q	R	S	A	B	C	D
0 – 7.5	0	0	1	1	0	1	0	0
7.5-15	0	0	1	1	0	1	0	0
15 – 22.5	0	1	1	0	0	0	1	0
22.5 – 30	0	1	1	0	0	0	1	0
30 – 37.5	1	1	0	0	0	0	0	1
37.5 - 45	1	1	0	0	0	0	0	1
45 – 52.5	1	0	0	1	1	0	0	0
52.5 - 60	1	0	0	1	1	0	0	0

4.3 Comparison of Inductance Values

Table 3: Comparison of Inductance Values at 5.2 A

Inductance (in mH)	Calculated	Measured	FEA
L_{amax}	165	162.525	167.805
L_{amin}	61.53	63.38	68.02

A comparison of inductances by three different methods at fully aligned and fully unaligned positions is given in table 3, at rated phase current. In the fully aligned rotor position, both the analytical and finite element results are very close to the measured inductance values with 1.52% and 1.7%error respectively. On the other hand, in the fully unaligned rotor position, both the analytical and finite element results have the errors of 23% and 32.1% respectively. The error is attributable to the end effects, and the distortion of the magnetic properties of the core material due to punching stresses, inexact B-H characteristics provided by the steel manufacturers and inappropriate selection of the polynomial for B-H curve. End leakage effects are severe in the fully unaligned position because the reluctance of the end paths become comparable to that of the air gap paths. Even though the end effect has been included in the analytical method, the accurate modelling of the three dimensional geometry of leakage flux tubes is difficult. It is seen that the analytical results are closer to the measurement than the results of the finite element analysis.

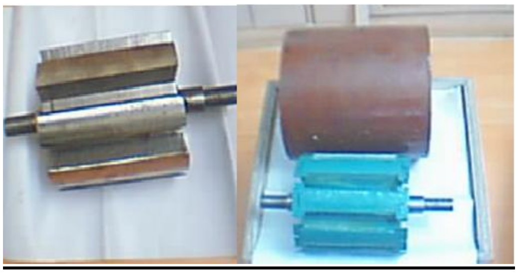

Fig15: Rotor & Stator of SR hub motor Prototype

5. CONCLUSION

A SR hub motor has been designed with the following dimensions and material data

No. Of stator Poles:	8
No. of Rotor poles:	6
Stator outside diameter:	233 mm
Rotor Bore diater:	165 mm
Core length:	75 mm
Air gap length:	1 mm
Back iron width:	17 mm
Number of turns/Phase	236
Stator pole arc:	0.384 rad
Rotor pole arc:	0.4189 rad
Steel:	m 19
SWG:	18

A prototype of the motor with exterior structure has been fabricated and can be incorporated within the wheels of a low speed electric vehicle. A simple, cost effective, low resolution position sensor is fitted to the machine. Using an asymmetric bridge converter configuration and the position sensor, excitation to the windings are offered in a sequence and the machine is run. It is found that the analytical, finite element and measured values of unaligned and aligned inductances are nearly equal.

ACKNOWLEDGEMENT

This work is carried out with the grant-in-aid received from All India Council for Technical Education, New Delhi, India, vide F.No.8023/RID/BOR/RPS-58/2005-06

REFERENCES

1. Arumugam, R., Lindsay, J.F. and Krishnan, R., "Sensitivity of Pole Arc/Pole Pitch ratio on Switched Reluctance Motor Performance", Proc. IEEE IAS Ann. Mtg., pp., Pittsburgh, Oct. 1988.
2. 2. Krishnan , R., Arumugam, R. and Lindsay, J.F., "Design Procedure for Switched Reluctance Motors" , IEEE Transactions on Industry Applications, vol.24, No.3, pp. 456-461, May/June 1988.
3. Miller T J E., Switched Reluctance motor drives a nd their control, Magna Physics Publishing and clarendons Press, Oxford, 1993.
4. Low T.S., Lin.H., Chen.S.X., Chang.K.T., Design and analysis of four phase (In-hub) mini-switched reluctance motor for spindle motor in hard disc drive, Proceedings of International Conference on Power Electronics and Drive Systems, 1995, pp 645 – 650, Vol. 2
5. Krishnan, R., "Switched Reluctance Motor Drives: Modeling, Simulation, Analysis, Design, and Applications", CRC Press, 2001.
6. Praveen Vijayaragavan, "Design of Switched Reluctance Motors and Development of a Universal Controller for Switched Reluctance and Permanent Magnet Brushless DC Motor Drives", PhD Thesis ,2001.
7. Mi-Ching Tsai, Chien-Chin Haung, Zheng-Yi Haung, A new two-phase homopolar switched reluctance motor for electric vehicle applications, Journal of magnetism and magnetic materials, No. 267, 2003, pp 173 – 181.
8. Jawad Faiz, K.Moayed-Zadeh, Design of switched reluctance machine for starter/generator of hybrid electric vehicle, Electric power systems research, No. 75, 2005, pp 153- 160.
9. Pandey.K., Rajagopal.K.R., Novel pole shapes for improved performance of SR hub motors, Digests of the IEEE
10. International Magnetics Conference, INTERMAG2005, PP 745 – 750.
11. 10. V.Radun, Design Considerations for Switched Reluctance Motor, IEEE Transactions on Industry Applications, Vol.31, No. 5, September/October, 1995.
12. 11. K.Cakir, A.Sabanovic, In-Wheel motor design for electric vehicles, 9th International workshop on Advanced Motion control, 2006, pp 613 – 618.
13. 12. David Cajander, Hoang Le-Huy, Design and optimization of a torque controller for a switched relctance motor drive for electric vehicles by simulation, Journal of Mathematics and computers in simulation, Vol No. 71, 2006, pp 333 – 344.
14. 13. Chia-Chang Tong, Wu-Shun Jwo, An assist-mode hybrid electric motorcycle, Journal of power soures, 174, 2007, pp 61 – 68.
15. 14. Ali Emadi, Young Joo Lee, Kaushik Rajashekara, Power Electronics and Motor Drives in Electric, Hybrid, and Plug-in Hybrid Electric Vehicles, IEEE Transactions on Industrial Electronics, Vol 55, No. 6, June 2008
16. 15. D.Xue, J.K.Lin, Z.Zhang, T.W.NG,K.F.Luk, K.W.Cheng and C.Cheung "Study of Motoring operation of In-Wheel Switched Reluctance Motor Drives for Electric Vehicles" International Conf., on Power Electronics and Applications, 2009
17. Sakthivel, P.; Chandrasekar, V.; Arumugam, R.; Design of a 250w, low speed switched reluctance Hub motor for two wheelers Electrical Energy Systems (ICEES), 2011 1st International Conference on 2011 , Page(s): 176 – 181
18. Roger C, Becerra, Mehrdad Ehsani, Commutation of SR motors, IEEE Transactions on Power Electronics, Vol.8, No. 3, July 1993.